

# Accuracy of rendered depth in head-mounted displays: role of eyepoints location

L. Vaissié and J. P. Rolland

School of Optics-CREOL  
University of Central Florida, Orlando FL 32816

## ABSTRACT

Eyetracking is typically not available in head-mounted displays, and eye motions are thus simply ignored when 2D virtual images are displayed, giving rise to rendered depth errors in generating stereoscopic image pairs in head-mounted displays. We present an investigation and quantification of rendered depth errors linked to natural eye movements in binocular head-mounted displays, or Albertian errors, for three possible eyepoint locations: the center of the entrance pupil, the nodal point, and the center of rotation. Theoretical computations based on the intersection of chief rays concluded that, while the center of rotation yields minimal depth errors if no eyetracking is used, rendered angular errors may in some cases be significant (i.e. up to six degrees). Based on the analysis presented in this paper, we suggest that the center of entrance pupil be chosen for far field applications. The center of rotation of the eye should be chosen for near field applications under the assumption that they emphasize position accuracy versus angular accuracy. Preventing or minimizing rendered depth errors may be required for some high accuracy tasks related, for example, to medical or military visualization.

**Keywords:** head-mounted displays, rendered depth, eyepoint, Albertian errors, eyetracking

## 1. INTRODUCTION

In today's information intensive environment, it is necessary to collect, process, and display accurate data from a variety of external sources so experts across various disciplines are able to make critical decisions in dynamic presentation of information. Such contexts require that 3D data be rendered accurately and that remaining errors be quantified.

The military for example is interested in the development of head-mounted displays (HMD) that can accurately display information to increase visual awareness for detection, identification, and tracking of objects of interest, as well as reduce cognitive demand, improve navigation maneuvers, and increase acceptability for closed hatch operations. The medical and biomedical fields face similar challenges and require high-end technology for training and computer-guided surgery tools for example.

The goal of this paper is to provide a comprehensive understanding of the impact of different settings for the eyepoints location on rendered depth errors in head-mounted displays. As part of the investigation, we quantify the types and magnitude of rendered depth errors, at and surrounding the gaze point, based on standard methods for the generation of stereoscopic image pair.

## 2. STEREOSCOPIC MAPPING TECHNIQUE: THE ORIGIN OF ALBERTIAN ERRORS

The mapping technique used to create stereoscopic images in HMDs is based on the principle of Alberti's window<sup>1</sup> that requires the eye to be reduced to a single point referred as the *eyepoint*. A 3D object in the virtual environment is projected into two 2D images, each generated from an eyepoint associated with each eye. Thus, a point rendered in the virtual environment maps to two points, one in each 2D image. A point on a 3D object is therefore rendered to appear at the crossing of rays joining the eyepoints and the mapping points in the 2D stereoscopic images.

### **2.1 Eyepoints location in the case of eyetracking capability**

If the motion of the eyes is tracked, the centers of the entrance pupils that delineates the centroids of energy on the retina from a point of light, constitute the correct eyepoints for rendering depth in virtual environments as first pointed out by Ogle and later stressed by Rolland.<sup>5-6</sup> Ogle specifically pointed out that the chief rays, that go through the centers of the entrance pupil of the eyes, should be used to determine the location of the apparent point in stereoscopic devices instead of the visual lines that go through the nodal points.

It is thus reasonable to assume that a point in virtual space will be perceived at the intersection of the two rays issued from the centroid of energy on the retina and passing through the centers of the entrance pupils. These rays are chief rays assuming that non-symmetric image point degradations are negligible compared to the defocus of the point on the retina. We will use here this model of perception through the intersection of chief rays for our investigation. We will further discuss the conditions under which such an intersection exists, as we discovered that it is not always the case.

### **2.2 Three suggestions for the eyepoints under no eyetracking capability**

In the case of no eyetracking capability, because the eyepoints are assumed to remain motionless during the perception of virtual objects, rendered depth errors are created. The magnitude of such errors is quantified in this paper as a function of the eyepoints locations considered to be either the entrance pupils of the eyes, the nodal points, or the centers of rotation of the eyes.

The choice of the entrance pupils of the eyes even when no eyetracking capability comes as perhaps a natural choice given these points are the eyepoints giving no rendered depth error in the case of eyetracking. We shall in fact demonstrate that they can be the best choice under certain visualization schemes.

The nodal points have been used in the stereoscopic vision literature to describe the Vieth-Müller circle which is the locus of points in space that project images to corresponding points in the two retinas for a given position of the eyes.<sup>2</sup> The well-known unit angular magnification at these points appears convenient for mapping the 2D virtual images to the retina, and the nodal points are therefore commonly used in computer graphics as the eyepoints.

It has been suggested however in the literature for visual instrumentation to consider the centers of rotation of the eyes instead of the centers of the entrance pupils as the eyepoints.<sup>3</sup> In this case, the computational model for stereo pair generation ensures that there is no rendered depth error at the gaze point of the HMD user. Indeed, the interocular distance, measured between the centers of rotation of the eyes, remains fixed with eye movements and equal user's IPD measured for infinity viewing. This choice appears to solve the problem of having to dynamically adjust the centers of perspective projection to constantly register the user's graphical eyepoints, a procedure that would require measuring of eye movements. Furthermore, it has been suggested that selecting the centers of rotation of the eyes as the eyepoints could serve as an alternative to eyetracking.<sup>4</sup>

The investigation of the type and magnitude of rendered depth errors according to the choice of eyepoints location presented here will clarify the role of eyetracking in HMDs for accurate rendered depth, whether the eyepoints are chosen to be at the center of rotation of eyes or elsewhere.

### **2.3 Natural convergence motion of the eyes**

The fixed eyepoints assumption used for mapping stereoscopic images to a 3D object was highlighted as a possible factor of rendered depth errors in virtual environments. It is well known that the eyes rotate towards the gaze point in order to avoid diplopic images.<sup>7</sup> As the eyes rotate, the centers of the entrance pupils move accordingly. Thus the rays used to render a point in the virtual environment do not generally coincide with the chief rays used to perceive this point because of the rotation of the eyes. This phenomenon is related to the loss of alignment with motion of the eye or ocular parallax described by Brewster.<sup>2</sup> These types of errors are known as Albetian errors.<sup>8</sup>

In this investigation, we will only take into account the rotations of the eyes, neglecting the small translation motions during convergence. We will also consider HMDs without eye tracking capability. If eye tracking was performed, it would serve to remove rendered depth errors by determining the location of the centers of the entrance pupils of the eyes and use them as the eyepoints locations to render virtual environments in real time.

### 3. RENDERED DEPTH ERROR DERIVATION

Given an eyepoint for rendering, the location of a rendered point is the intersection of the lines mapping the eyepoints to the relevant mapping points in the displayed stereoscopic images as shown in Figs.1 and 2. The location of the apparent point is then derived considering the intersection of the chief rays joining the rotated centers of the entrance pupils after convergence to the gaze point and the mapping points as shown in Fig.2. We quantify rendered depth error by computing the angular error between an apparent and a rendered point in a fixed frame of coordinates for different eyepoints and HMDs configurations. We will use the angles of elevation and azimuth referred to in the vision literature to parameterize the problem.<sup>2</sup>

#### 3.1. Notations and definition of the framework

We use a frame of coordinates  $X, Y, Z$  centered on the interocular axis midway called the cyclopean point as shown in Fig.1. The interocular axis is taken to pass through the centers of rotation of the eyes so that the axes remain a still reference when the eyes rotate. This enables investigating different eyepoints with a common fixed reference. The  $XZ$  plane is taken to be the horizon plane.

Given any point  $P$  in this frame, its  $x, y, z$  coordinates will be expressed as a function of  $\phi_p$ , the cyclopean elevation angle,  $\theta_p$  and  $\theta'_p$  the azimuth angles, and  $\alpha$  the oculocentric elevation angle between the plane of regard and the binocular plane defined in Fig.1. The elevation angle between the horizon plane and the plane of regard is  $\phi_g$ .

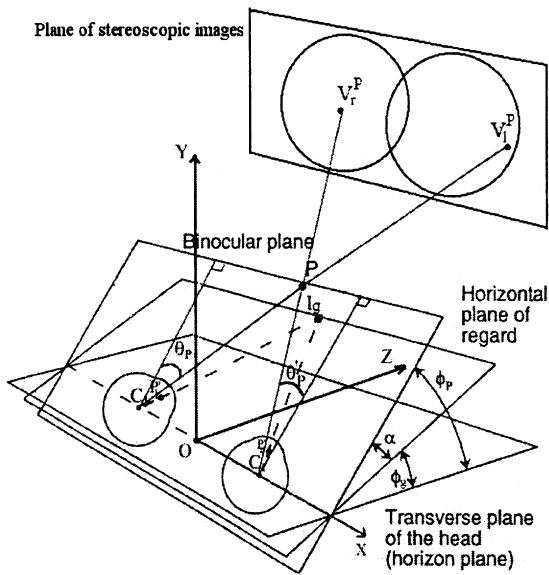


**Fig.1:** Definition of the frame of coordinates. The center of the set of axis is the cyclopean point  $O$ , located on the inter-ocular axis midway. The  $XZ$  plane is the horizon plane. A point  $P$  rendered in the 3D environment is defined by the azimuth angles  $\theta_p$ ,  $\theta'_p$  and by the elevation angle  $\phi_p$  of its mapping points  $V_l^P$  and  $V_r^P$ . The binocular plane is defined by  $\phi = \phi_p$ .

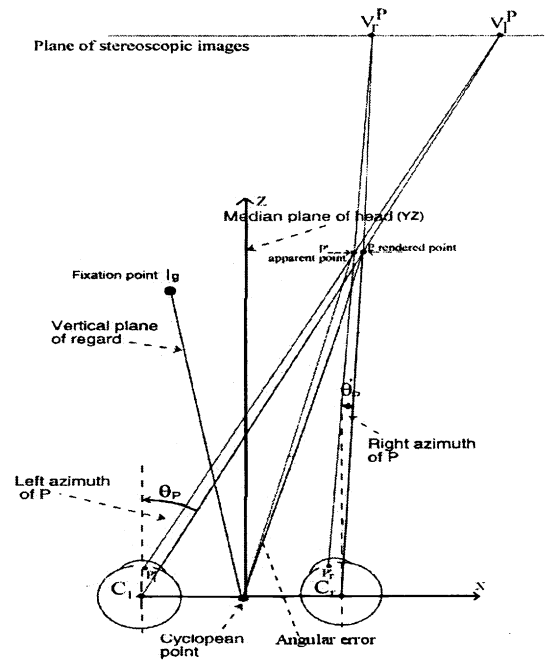


**Fig.2:** Top view of the stereoscopic vision model presented in Fig.1. The location of the apparent versus rendered point is shown. The angular error is defined as the visual angle from the cyclopean point. The mapping points  $V_l^P$  and  $V_r^P$  are displayed in the plane of stereoscopic images. Those points are used to derive the location of the apparent point as the intersection of the chief rays. The chief rays go through the rotated centers of the entrance pupil  $P'_r$  and  $P'_l$  when the user gazes to  $I_g$ .

Let  $I_g(x_g, y_g, z_g)$  be the fixation point in this frame of coordinates. The gaze point is located at the intersection of the imaginary lines joining the eyepoints to the corresponding mapping points  $V_l^g(x_l^g, y_l^g, z_l^g)$  and  $V_r^g(x_r^g, y_r^g, z_r^g)$  displayed in the 2D virtual images respectively for the left and the right eye. We consider that  $z_l^g = z_r^g = D$  which means both stereoscopic virtual images are displayed in the same plane at a distance  $D$  from the interocular axis. This plane is perpendicular to the horizon plane.

The computations that follow investigate the perception errors on a point rendered at  $P(x_g + dx, y_g + dy, z_g + dz)$  when the user gazes to  $I_g$ . The investigation of rendered depth error for the gaze point is a particular case of the general computation for  $dx = dy = dz = 0$ . The  $P$  coordinates are eyepoint-dependent and are given by the intersection of  $E^l V_P^l$  and  $E^r V_P^r$ . The parameter  $d$  is the algebraic distance between the center of rotation of the eye and the eyepoint.

The convergence motion towards the gaze point  $I_g$  leads to a rotation of the eyes. Consequently, the centers of the entrance pupils, named  $P_l$  and  $P_r$  respectively for the left and right eyes, rotate to  $P'_l$  and  $P'_r$ . Thus the rendered point  $P$  is actually perceived in  $P'$ , intersection of the chief rays  $P'_l V_P^l$  and  $P'_r V_P^r$ .

We then quantify the rendered depth error as the angular error for the cyclopean point  $O$ , given by

$$\text{AngE} = \frac{\mathbf{OP} \cdot \mathbf{OP}'}{\|\mathbf{OP}\| \|\mathbf{OP}'\|} = \frac{(x'_P x_P) + (y'_P y_P) + (z'_P z_P)}{\sqrt{(x'_P)^2 + (y'_P)^2 + (z'_P)^2} \cdot \sqrt{(x_P)^2 + (y_P)^2 + (z_P)^2}} \quad (1)$$

The function  $\text{AngE}$  depends upon the parameters  $\alpha, \theta_P, \theta'_P, \theta_g, \theta'_g, \phi_g, d, D$ .

### 3.2 Coordinates of the rendered point P

The coordinates of the mapping points  $V_l^P$  and  $V_r^P$  are respectively given by

$$V_l^P \left( \frac{D \cdot \tan \theta_P - C_l C_r}{\cos \phi_P}, D \cdot \tan \phi_P, D \right) \quad \text{and} \quad V_r^P \left( \frac{D \cdot \tan \theta'_P + C_l C_r}{\cos \phi_P}, D \cdot \tan \phi_P, D \right) \quad (2)$$

The rendered point  $P$  is located at the intersection of  $E^l V_P^l$  and  $E^r V_P^r$ . Thus its coordinates satisfy the system

$$\begin{cases} E^l P = k \cdot E^l V_P^l \\ E^r P = k' \cdot E^r V_P^r \end{cases}, \quad (k, k') \in \mathfrak{R}^2 \quad (3)$$

Using Thales theorem in the parallelogram  $E^l E^r V_P^l V_P^r$ , one can show

$$k = k' = \frac{C_l C_r \cdot \cos(\phi_P)}{D \cdot (\tan \theta_P - \tan \theta'_P)} \quad (4)$$

Thus the system (3) yields

$$\begin{cases} x_P = \frac{C_l C_r}{2} + \frac{C_l C_r \cdot \tan \theta'_P}{(\tan \theta_P - \tan \theta'_P)} \\ y_P = \frac{C_l C_r \cdot \sin \phi_P}{(\tan \theta_P - \tan \theta'_P)} \\ z_P = d + \frac{C_l C_r \cdot \cos \phi_P}{D \cdot (\tan \theta_P - \tan \theta'_P)} \cdot (D - d) \end{cases} \quad (5)$$

### 3.3 Coordinate of the centers of the entrance pupils

The convergence motion of the eyes can be described as a composition of two successive rotations  $\theta_g$  and  $\phi_g$ . The centers of the entrance pupil then rotate from the horizon plane to the plane of regard by these rotations. The coordinates of the rotated center of the entrance pupil  $P'_l$  are therefore

$$\mathbf{OP}'_l = \begin{pmatrix} r \sin \theta_g - \frac{C_l C_r}{2} \\ r \cos \theta_g \cdot \sin \phi_g \\ r \cos \theta_g \cdot \cos \phi_g \end{pmatrix} \quad (6)$$

where  $r$  is the distance between the center of rotation and the center of the entrance pupil of the eye. In the same way the coordinates of  $P'_r$  are

$$\mathbf{OP}'_r = \begin{pmatrix} r \sin \theta'_g + \frac{C_l C_r}{2} \\ r \cos \theta'_g \cdot \sin \phi_g \\ r \cos \theta'_g \cdot \cos \phi_g \end{pmatrix} \quad (7)$$

### 3.4 Conditions for an intersection of the chief rays in 3D

The location of the apparent point  $P'$  is determined by deriving the coordinates of the intersection of the chief rays  $P'_l V_l^P$  and  $P'_r V_r^P$ . This statement points to a problem inherent in the mapping technique: in the 3D virtual environment the location of the apparent point may be derived only if the chief rays cross. This condition requires  $P'_l P'_r$  and  $V_l^P V_r^P$  to be coplanar. We shall treat first the case where the mapping points of the apparent point lie in the plane of regard, this case satisfying the coplanarity condition. We will then derive the conditions required on the fixation point if the mapping points of the apparent point are not included in this plane.

#### 3.4.1 Case 1: $V_l^P$ and $V_r^P$ are in the plane of regard.

If  $V_l^P$  and  $V_r^P$  lie in the plane of regard, there is an intersection of the chief rays. The condition on the elevation angle is  $\phi_g = \phi_P$ . The apparent point  $P'$  will then be rendered in the plane of regard. However, the rendered point  $P$  is not necessarily included in the plane of regard but in the plane formed by its mapping points and the eyepoints. If  $\phi_g = \phi_P$  there will be an intersection of the chief rays wherever the gaze point may lie in the plane  $\phi = \phi_g$ .

#### 3.4.2 Case 2: $V_l^P$ and $V_r^P$ are not in the plane of regard.

If  $V_l^P$  and  $V_r^P$  are not included in the plane of regard, the chief rays intersection exists if and only if  $P'_l P'_r$  is parallel to  $V_l^P V_r^P$ . Since  $C_l C_r$  is parallel to  $V_l^P V_r^P$  by definition of the mapping points, the vectors  $P'_l P'_r$  and  $V_l^P V_r^P$  are then coplanar if  $P'_l P'_r \times C_l C_r = 0$ , where  $\times$  denotes the cross product of two vectors. This condition leads to  $|\theta_g| = |\theta'_g|$ . The solution  $\theta_g = \theta'_g$  leads to  $P'_l C_l$  parallel to  $P'_r C_r$  which means there is no possible intersection of

the chief rays. Therefore the condition required for a chief rays intersection is  $\theta_g = -\theta'_g$ . Consequently the plane  $x = 0$  is the only solution for the gaze point which corresponds to the median plane of the head. If it is not the case, the chief rays do not cross and the location of the apparent point cannot be derived as the simple intersection of two rays.

### 3.5 Derivation of the apparent point coordinates

We now assume that we operate under intersection of chief rays. The apparent point  $P'$  is thus located at the intersection of  $P'_1 V_1^P$  and  $P'_r V_r^P$ . Its coordinates are then solution of the system of equations

$$\begin{cases} P'_1 P' = k \cdot P'_1 V_1^P \\ P'_r P' = k' \cdot P'_r V_r^P \end{cases} \quad \text{with } (k, k') \in \mathfrak{R}^2 \quad (8)$$

By matching the  $x_p$  and  $z_p$  expressions in (8), one finds that the coefficients  $k$  and  $k'$  satisfy the system

$$\begin{pmatrix} c \\ d \end{pmatrix} = M \cdot \begin{pmatrix} k \\ k' \end{pmatrix} = \begin{pmatrix} a & b \\ a' & b' \end{pmatrix} \begin{pmatrix} k \\ k' \end{pmatrix} \quad (9)$$

where

$$\begin{cases} c = r(\sin \theta'_g - \sin \theta_g) + C_1 C_r & a = \frac{D \cdot \tan \theta_p}{\cos \phi_p} - r \sin \theta_g & b = -(D \cdot \tan \theta'_p - r \cdot \sin \theta'_g) \\ d = r \cos \phi_g \cdot (\cos \theta'_g - \cos \theta_g) & a' = D - r \cos \theta_g \cdot \cos \phi_g & b' = -(D - r \cdot \cos \theta'_g \cdot \cos \phi_g) \end{cases} \quad (10)$$

The solutions are therefore given by

$$k = \frac{-d \cdot b + e \cdot c}{\det(M)} = \frac{-d \cdot b + e \cdot c}{a \cdot b' - a' \cdot b} \quad (11.1)$$

$$k' = -\frac{c \cdot b' - a \cdot d}{\det(M)} = -\frac{c \cdot b' - a \cdot d}{a b' - a' b} \quad (11.2)$$

We then obtain the coordinates of the apparent point  $P'$  as a function of the azimuth and elevation angles of the rendered point and the gaze point, by replacing  $k'$  by its expression given in (11.2). To give more insight for numerical applications, it is possible to replace  $\phi_p$  by  $(\phi_g + \alpha)$  to express the coordinates of  $P'$  as a function of the oculocentric elevation angle between the binocular plane and the plane of regard. The expression of  $P'$  using (8) and (11.2) is then

$$\begin{cases} x'_p = r \sin \theta'_g + \frac{C_1 C_r}{2} + k' \left( \frac{D \cdot \tan \theta'_p}{\cos(\phi_g + \alpha)} - r \sin \theta'_g \right) \\ y'_p = r \cos \theta'_g \cdot \sin \phi_g + k' \cdot (D \cdot \tan(\phi_g + \alpha) - r \cos \theta'_g \cdot \sin \phi_g) \\ z'_p = r \cos \theta'_g \cdot \cos \phi_g + k' \cdot (D - r \cos \theta'_g \cdot \cos \phi_g) \end{cases} \quad (12)$$

## 4. PARAMETERS USED FOR NUMERICAL QUANTIFICATION

### 4.1 Model of the eye

We used the numerical features of the “schematic” eye proposed by Gullstrand.<sup>29</sup> The entrance pupil is the image of the iris through the refracting surface of the cornea. The distance between the center of the entrance pupil and the vertex of the cornea is found to be 3mm. The distance between the center of rotation and the vertex of the cornea is 12.25mm. Thus the parameter  $d$  is taken to be 9.25mm when the center of the entrance pupil is taken to be the

eyepoint and 0 when the center of rotation of the eye is the eyepoint. The parameter  $r$  equals 9.25mm by definition. The interocular distance is taken to be 65mm.

#### 4.2 HMDs set-ups investigated

Two common setups for HMD design were selected as they represent two extreme configurations: far field visualization as opposed to near field visualization. Visualization of collimated targets in cockpits is a possible application of the far field configuration for military applications. Near field visualization may be used in medical visualization to superimpose data onto a patient's body during surgery. The parameter values are summarized in Table 1 according to the application considered.

**Table 1:** Parameters used for the investigation of near field and far field visualization

Parameter	Near field visualization	Far field visualization
D (m)	1	10
$z_g$ (m)	1	10
Vertical FOV ° ( $\alpha$ )	+45	+45
Horizontal FOV ° ( $ \theta_p - \theta_g $ )	40	40

### 5. NUMERICAL QUANTIFICATION OF ALBERTIAN ERRORS

The results are presented following the two possible cases of getting an intersection of the chief rays as defined in section 3. For each case, quantification of errors for far field and near field HMD configuration is illustrated. The eyepoint is only taken to be the center of rotation of the eye or the center of the entrance pupil. It is possible to quantify the error resulting from choosing the nodal point as the eyepoint as an average of the error amplitudes presented here for the two other eyepoints.

#### 5.1 Case 1: $V_l^P$ and $V_r^P$ are in the plane of regard

This case allows investigating the contribution on rendered depth errors of the gaze point shift with respect to the median plane of the head. The parameter  $\phi_g$  is set to zero (i.e.  $y_g = 0$ ) because the coplanarity of  $I_g, V_l^P, V_r^P$  and the eyepoints makes the error invariant with respect to the elevation angle if the eyepoint is the center of rotation of the eye. If the eyepoint is the center of entrance pupil is the eyepoint the error dependence upon the elevation angle is negligible.

Thus, given  $z_g$  and D fixed for near or far field configurations, we present a quantification of the angular error (1) on rendered point P as a function of  $\theta_p, \dot{\theta}_p$  and  $\theta_g$ . The variation of the gaze point azimuth angle  $\theta_g$  is taken to be +- 20 degrees. The angle  $\dot{\theta}_g$  is then set accordingly. We consider that the head would rotate for larger variations of the gaze point location. The variation of  $\theta_p$  and  $\dot{\theta}_p$  is defined by the field of view (+- 40 degrees).

##### 5.1.1 Far field visualization

In a far field configuration, stereoscopic images are collimated (D=10m) and the gaze point lies in the plane  $z = z_g = 10m$ . We successively investigate rendered depth errors for the eyepoint taken to be the center of rotation ( $d = 0$ ) and the center of the entrance pupil of the eye ( $d = r = 9.25mm$ ).

The centers of rotation of the eye as the eyepoints. The results are displayed in Fig. 3. The minimum error is obtained around  $\theta_p = \theta'_p$ . In this case, the symmetry of the mapping points of P with respect to the eyepoints decreases the angle disparity between apparent and rendered point. The error remains below  $1^\circ$  for rendered points within  $|\theta_p - \theta_g| < 10^\circ$  and  $|\theta'_p - \theta_g| < 10^\circ$ . The error increases slightly with respect to  $\theta_g$ . The maximum of angular error is  $2.3^\circ$  for  $\theta_g = 0^\circ$ , and  $3.5^\circ$  for  $\theta_g = 20^\circ$ .

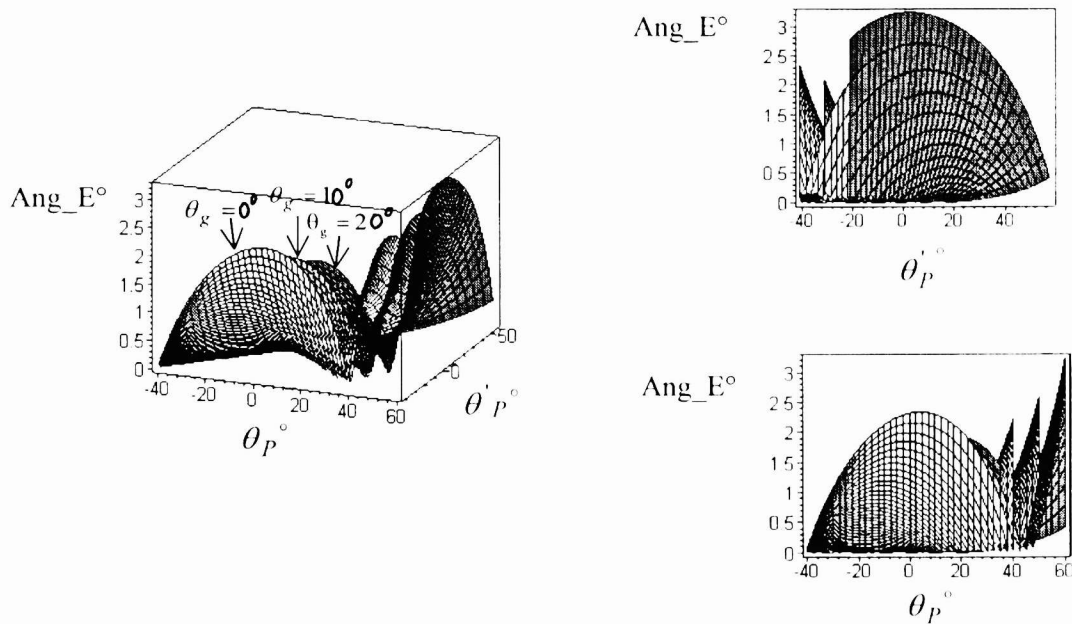


**Fig.3 :** The center of rotation is the eyepoint. The angular error is plotted as a function of  $\theta'_p$  and  $\theta_p$  for different  $\theta_g$  angles. The z coordinate of the gaze point is set to 10m and the stereoscopic images are collimated ( $D = z_g = 10m$ ) for far field configuration. The mapping points of P and the gaze point lie in the plane of regard defined by  $\phi_g = 0$ .

The centers of the entrance pupils as the eyepoints. The error magnitude is highly dependent upon the location of the gaze point. If the gaze point is around the median plane of the head, the angular error is negligible ( $< 0.005^\circ$ ) but if  $\theta_g = 20^\circ$  then the error reaches 3.5 degrees for points rendered at 40 degrees azimuth away from the gaze point. The maximum error is obtained for points rendered close to the eyes. The error, represented as a surface function of  $\theta_p$  and  $\theta'_p$  may be approximated by a plane of equation  $AngE = \beta(\theta_p - \theta'_p)$  where  $\beta$  is found to be  $2.5 \times 10^{-3} \theta_g$  (with  $\theta_g$  in degrees).

### 5.1.2 Near field visualization

In a near field configuration, stereoscopic images are displayed at arm length distance and the gaze point lies in the plane  $z = z_g = 1m$ . The error is found to vary in the same way as found for far field configuration. The error magnitudes are also equivalent.

### 5.2: Case 2 $V_l^P$ and $V_r^P$ are not in the plane of regard

Let's consider the gaze point is now fixed in the median plane of the head. The elevation angle was set to 0 for numerical quantification. We investigate rendered depth errors for points P rendered in planes  $x_p = k$  called k-

planes,  $0 < k < 50\text{cm}$ . Thus, one can derive from (5) a relation to define  $\theta_p'$  as a function of  $\theta_p$  when P is in the  $k$ -plane. This relation is

$$\tan \theta_p' = \frac{k - \frac{IA}{2}}{k + \frac{IA}{2}} \cdot \tan \theta_p \quad (13)$$

Thus, given a  $k$ -plane, an eyepoint and a near field or far field configuration, the angular error (1) is plotted as a function of  $\theta_p$  and  $\alpha$  in Fig.4. This enables, for a fixed gaze point, to evaluate errors for points rendered in a ( $80^\circ$  Horizontal  $90^\circ$  Vertical) field of view specified in table 1.

### 5.2.1 Far field visualization

*The center of rotation is the eyepoint.* The results are displayed in Fig.4. The error reaches zero for the very particular case when the apparent point is located at the gaze point. This recalls that the center of rotation does not lead to perception errors on the gaze point. The error is maximum for points rendered close to the eyes ( $\theta_p = 40^\circ$ ) and for large elevation angle  $\alpha$ . The error happens to be highly dependent upon  $\alpha$  when the  $k$ -plane is close to the median plane of the head. When the point is rendered in a plane such that  $x_p > 15\text{cm}$  the error does not exceed  $1.8^\circ$ . However it reaches  $6^\circ$  if the plane is less than  $2\text{cm}$  from the median plane of the head. This is due to the direction of the vector  $\mathbf{PP}'$  that happens to be almost vertical when the mapping points of P are displayed symmetrically with respect to the median plane of the head. For a given  $\alpha$ , the error does not vary sharply with  $\theta_p$ . The minimum error is obtained for points rendered around the gaze point and the error remains below  $1^\circ$  if  $|\theta_p| < 20^\circ$  and  $|\alpha| < 10^\circ$ .

*The center of the entrance pupil is the eyepoint.* The variation of the error is found to be similar to the former case. However the magnitude of the error is much lessened. It never exceeds  $0.005$  degrees for any point rendered in the given FOV.

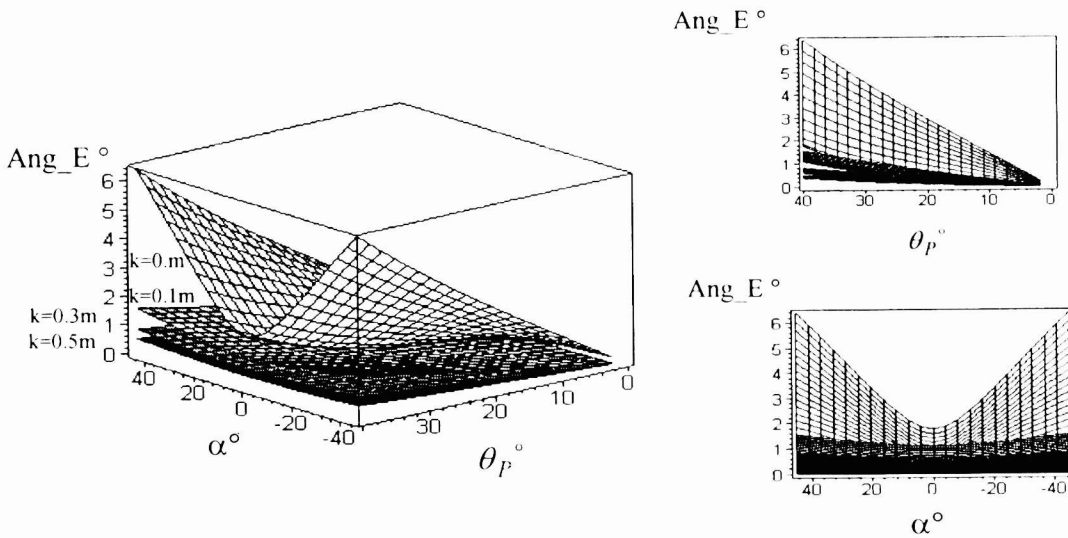


**Fig.4:** The center of rotation is the eyepoint. Angular error is plotted as a function of  $\alpha$  and  $\theta_p$ . The rendered points lie in a plane  $x_p = k$ . The stereoscopic images are collimated ( $D = z_g = 10\text{m}$ ) for far field configuration. The gaze point is in the median plane of the head. The FOV investigated is ( $80^\circ$  horizontal,  $90^\circ$  vertical), the plot only shows ( $40^\circ, 90^\circ$ ) FOV for reasons of symmetry.

### 5.2.2 Near field visualization

*The center of rotation is the eyepoint.* The error varies similarly to the far field configuration.

*The center of the entrance pupil is the eyepoint.* The variation of the error as a function of  $\alpha$  and  $\theta_p$  is similar to the far field case. Higher magnitude is found for near field configuration although it does not exceed 0.04 degrees.

## 6. DISCUSSION AND CONCLUSION

We have presented an investigation of the choice of the eyepoints location in binocular HMDs, as they relate to rendered depth errors. We showed that a simple geometrical model of 3D perception highlights the role of Albertian errors regarding accuracy of rendered depth in HMDs.

First, fixed eyepoints lead to a displacement and slight distortions of 3D virtual objects. By comparing the rendered depth errors for three eyepoints locations, the center of rotation benefits from not shifting the gaze point. It leads to the smallest error magnitude in the location of 3D virtual image. However, regarding the angular perception of objects around the gaze point, the center of rotation leads to the greatest error magnitude while the center of the entrance pupil does not yield tangible errors. It is therefore useful to decouple near field and far field applications.

For far field applications the center of the entrance pupil appears the best choice for the eyepoint. The angular error is negligible within a  $\pm 40^\circ$  FOV provided a  $\pm 10^\circ$  azimuth gazing angle range. The center of rotation leads to significant errors up to  $6^\circ$  in the same configuration. Beyond that range, all eyepoints give significant angular errors.

For near field configuration, the center of rotation may be the best choice for the eyepoint as it does not spatially shift the gazed 3D object like the center of entrance pupil does even though the angular error is greater for the former. This may be justifiable because absolute depth location is likely more important than angular accuracy for near field applications. Nevertheless it is important to note that the center of entrance pupil yields negligible angular errors ( $\leq 0.04^\circ$ ) within  $\pm 40^\circ$  elevation and azimuth if the gaze point is around the median plane of the head.

The choice of eyepoints should be task-dependent. For specific tasks where angular perception is more important than exact 3D location, such as target selection by jet pilots, the center of the entrance pupil should be chosen. In contrast, if absolute depth perception or stereopsis is critical, for applications such as surgery, then the center of rotation should be taken to be the eyepoint location.

Eyetracking provides the exact location of the center of the entrance pupil. Thus, all the errors would be corrected if mapping points were computed with respect to the rotated centers of the entrance pupils.

## ACKNOWLEDGMENTS

This work was supported by the National Institute of Health Grant 1-R29-LM06322-01A1, and a contract from ELF-Aquitaine France.

## REFERENCES

1. J.E. Cutting. *Perception with an eye for motion*. Bradford Book, MIT press, 1986.
2. I.P. Howard & B.J. Rogers. *Binocular vision and stereopsis*. Oxford psychologic series **29**, Oxford university press, 1995.
3. G.H. Fry. *Geometrical optics*, Chilton book company, 1969.
4. R.L. Holloway. *Registration errors in augmented reality systems*. PH.D. dissertation, department of computer science, university of North Carolina at Chapel Hill. 1994.
5. K.N. Ogle. *Spatial localization through binocular vision*. The eye, vol. **4**, Academic, New York, 409-417, 1962.

6. J.P. Rolland. "Head-mounted displays for virtual environments: the optical interface". Invited. International Lens Design Conference, Proceeding of OSA 22, 329-333 (1994).
7. J. Siderov, and R.S. Harwerth, "Precision of stereoscopic depth perception from double images", *vision res.* **33** (11), 1553-1560 (1993).
8. J. P. Wann, S. Rushton, M. Mon-Williams, "Natural problems for stereoscopic depth perception in virtual environments". *Vision res.*, **35**, p. 2731-2736.
9. R.S. Longhurst. *Geometrical and physical optics*. New York: Longmann. 1973.
10. W. Robinett, and J. P. Rolland, "A computational model for the stereoscopic optics of a head-mounted display", *Presence: Teleoperators and Virtual Environments* (MIT Press), **1**:1,45-62 (1992).
11. C. Deering. *High resolution virtual reality*. *Computer Graphics*, **26**, 2. 1992.
12. D. B. Diner and D.H. Fender. *Human engineering in stereoscopic viewing devices*, Plenum Press New York and London, 1993.
13. K.N. Ogle. *Spatial localization through binocular vision*. *The eye*, vol. **4**, Academic, New York, 409-417, 1962.
14. J.P. Rolland, W. Gibson. Towards quantifying depth and size perception in virtual environments. *Presence*, **4**, 1, 24-49. 1995
15. K.R. Boff and J.E. Lincoln. *Engineering Data Compendium: Human Perception and Performance*. AAMRL, Wright-Patterson AFB, OH. 1988.
16. J.P. Rolland. *Head-mounted displays for virtual environments: the optical interface*. International lens design conference, Proc. OSA **22**, 329-333. 1994
17. K.N. Ogle and P. Boeder. *Distortion of stereoscopic spatial localization*. *J. opt. Soc. Amer. B*, **38**, 723-733. 1948.
18. J.P. Rolland, A. Yoshida, L.D. Davis, J.H. Reif. *High-resolution inset head-mounted display*. *Applied optics*, **37**, 19, 4183-4193, 1998.
19. J.P. Rolland, M.W. Krueger, and A. Goon. *Multi-focal planes in head-mounted displays*. (to appear in *Applied Optics*, 2000).